

Synthesis, crystal structure and magnetic properties of a cyanide-bridged Fe^{III}–Mn^{III} bimetallic chain based on [Fe(bipy)(CN)₄][−] building block

Yan Xu^a, Xiao-Ping Shen^{a,*}, Hu Zhou^b, He-Qing Shu^a, Wenxian Li^c, Ai-Hua Yuan^b

^aSchool of Chemistry and Chemical Engineering, Jiangsu University, Zhenjiang 212013, PR China

^bSchool of Material Science and Engineering, Jiangsu University of Science and Technology, Zhenjiang 212003, PR China

^cInstitute for Superconducting & Electronic Materials, University of Wollongong, NSW 2522, Australia

ARTICLE INFO

Article history:

Received 15 November 2008

Accepted 20 January 2009

Available online 29 January 2009

Keywords:

Cyanide-bridged
Crystal structure
Magnetic properties
Iron
Manganese

ABSTRACT

A cyano-bridged bimetallic chain complex of [Mn(salen)][Fe(bipy)(CN)₄] (**1**) (salen = *N,N'*-ethylenebis(salicylideneiminato)dianion; bipy = 2,2'-bipyridine), which was prepared by self-assembly of [Fe(bipy)(CN)₄][−] and [Mn(salen)]⁺ ions, has been characterized by elemental analyses, ICP, IR, thermoanalysis, single crystal X-ray structure analysis and magnetic measurements. In complex **1**, each [Fe(bipy)(CN)₄][−] unit connects two [Mn(salen)]⁺ units with its two *trans*-cyanide groups, and each [Mn(salen)]⁺ unit is linked to two [Fe(bipy)(CN)₄][−] ions in *trans*-positions, resulting in a straight one-dimensional neutral chain structure of complex **1**. The chains are stacking via mainly the aromatic π–π-type interactions. Magnetic studies reveal the presence of weak antiferromagnetic interactions between the adjacent Fe^{III} and Mn^{III} ions through cyanide-bridges.

© 2009 Elsevier B.V. All rights reserved.

1. Introduction

In the past decade, much effort has been devoted to the study of the magnetic interactions and magneto-structural correlations in molecular systems for the purpose of exploiting new molecule-based magnetic materials and interesting multifunctional molecule-based material such as single-molecule magnets (SMMs), single-chain magnets (SCMs), high critical temperature magnetic materials, spin-crossover materials, and multifunctional materials [1–4]. It has been found that cyanide-bridged bimetallic assemblies, based on [M(CN)₆]^{*n*−} (M = Fe, Cr, Mn, Co) building blocks and hydrated metal ions [M'(H₂O)₆]^{*p*+} or unsaturated coordinated complex [M'(L)]^{*m*+}, possess extraordinarily excellent magnetic performance and form a family of magnetic materials [5–7]. Recently, as an alternative strategy, the employment of capped molecular entities [ML_{*p*}(CN)_{*q*}]^{*n*−} (L = polydentate ligand) instead of [M(CN)₆]^{*n*−} as building blocks have been studied by several research groups [8–12]. The existence of the ancillary ligand (L) in the building blocks plays a key role in controlling the directions of structural propagation, and, as a result, generates low-dimensional magnetic assemblies. Nowadays, A few series of bimetallic assemblies in this new family with interesting magnetic properties

such as SMM and SCM have been reported [13–16]. On the other hand, with enhanced Jahn–Teller effects and magnetic anisotropy, Mn^{III}–Schiff base complexes have been demonstrated as good precursors in constructing cyanide-bridged magnetic materials [17–21]. In our continuous efforts to assemble new cyanide-bridged magnetic complexes, we are now exploring the use of tailored cyanometalate complexes as building blocks. In the paper, we present a new cyanide-bridged chain complex [Mn(salen)][Fe(bipy)(CN)₄](**1**) obtained by assembly of a tailored cyanometalate complex of [Fe(bipy)(CN)₄][−] and a Mn^{III}–Schiff base complex of [Mn(salen)]⁺ (bipy = 2,2'-bipyridine; salen = *N,N'*-ethylenebis(salicylideneiminato)dianion)), and the magnetic and thermal properties of complex **1** were investigated.

2. Experimental

2.1. Physical measurements

Elemental analyses for C, H and N were performed at a Perkin-Elmer 240C microanalysis instrument (USA). Mn and Fe analyses were made on a Jarrell-Ash 1100+2000 inductively coupled plasma quantometer. IR spectra were recorded on a Nicolet FT-170SX spectrometer with KBr pellets in the 4000–400 cm^{−1} region. The thermoanalysis was measured by a NETZSCH STA449C differential scanning calorimeter. The magnetic measurements were per-

* Corresponding author. Tel.: +86 511 83593133; fax: +86 511 88791800.
E-mail address: xiaopingshen@163.com (X.-P. Shen).

formed using a Quantum Design MPMS-XL SQUID magnetometer. Diamagnetic corrections were made using Pascal's constants. Effective magnetic moments were calculated using the equation $\mu_{\text{eff}} = 2.828(\chi_M \times T)^{1/2}$, where χ_M is the magnetic susceptibility per formula unit.

2.2. Preparations

All chemicals and solvents were reagent grade and were used without further purification. The precursors of $\text{PPh}_4[\text{Fe}^{\text{III}}(\text{bipy})(\text{CN})_4] \cdot \text{H}_2\text{O}$ [22] and $[\text{Mn}^{\text{III}}(\text{salen})]\text{ClO}_4 \cdot 2\text{H}_2\text{O}$ [20,23] were synthesized according to the methods reported previously.

2.2.1. Caution

Perchlorate salts of metal complexes with organic ligands are potentially explosive and should be handled in small quantities with great care.

2.2.2. $[\text{Mn}(\text{salen})][\text{Fe}(\text{bipy})(\text{CN})_4]$ (**1**)

A solution of $[\text{Mn}^{\text{III}}(\text{salen})]\text{ClO}_4 \cdot 2\text{H}_2\text{O}$ (0.1 mmol) in methanol (10 ml) was added to a solution of $\text{PPh}_4[\text{Fe}(\text{bipy})(\text{CN})_4] \cdot \text{H}_2\text{O}$ (0.1 mmol) in acetonitrile (10 ml). The resulting solution was filtered and the filtrate was left to allow slow evaporation in dark at room temperature. Black crystals of complex **1** were obtained

after two days, washed with MeOH and H_2O , respectively, and dried in air. Anal. Found: C, 56.31; H, 3.51; N, 17.44; Fe, 8.80; Mn, 8.53%. Calcd. for $\text{C}_{30}\text{H}_{22}\text{FeMnN}_8\text{O}_2$: C, 56.54; H, 3.48; N, 17.58; Fe, 8.76; Mn, 8.62%. IR: $\nu_{\text{C}\equiv\text{N}}$ (cyanide): 2133, 2118 cm^{-1} .

2.3. X-ray crystallography

Diffraction data were collected at 291(2) K on a Bruker SMART APEX CCD area detector diffractometer using graphite-monochromated Mo-K α radiation ($\lambda = 0.71073 \text{ \AA}$) with the φ and ω scan mode. Empirical absorption correction was made with SADABS. The structure was solved by direct methods and refined by full matrix least-squares techniques based on F^2 . All non-hydrogen atoms were refined with anisotropic thermal parameters. The idealized positions of the hydrogen atoms were located by using a riding model. All computations were carried out using the SHELXTL-PC program package.

Crystal data for **1**: $\text{C}_{30}\text{H}_{22}\text{FeMnN}_8\text{O}_2$, $M = 637.35$, monoclinic, space group $P2(1)/c$ (No. 14), $a = 9.4749(7)$, $b = 21.2029(15)$, $c = 13.6263(10) \text{ \AA}$, $\beta = 92.262(1)^\circ$, $U = 2735.3(3) \text{ \AA}^3$, $Z = 4$, $D_c = 1.548 \text{ g/cm}^3$, $F(000) = 1300$, $\mu = 1.037 \text{ mm}^{-1}$ and $S = 1.01$. 14815 reflections measured, 5373 unique ($R_{\text{int}} = 0.037$). The final $R_1 = 0.0316$ and $wR_2 = 0.0830$ for 4129 observed reflections [$I > 2\sigma(I)$] and 379 parameters.

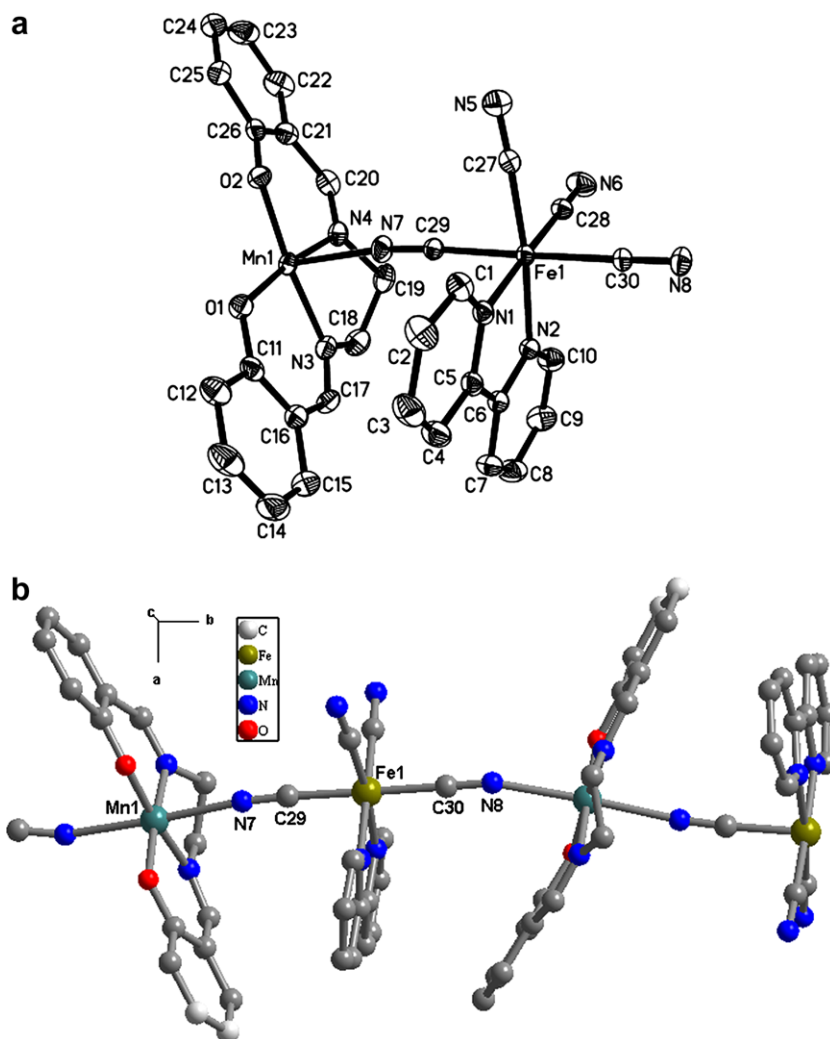


Fig. 1. Molecular view of complex **1** showing (a) the atom-labeling scheme and (b) bimetallic chain structure.

3. Results and discussion

3.1. Crystal structure

The structure of complex **1** is shown in Figs. 1 and 2. The selected bond distances and angles are listed in Table 1. The molecular structure of complex **1** consists of one $[\text{Fe}(\text{bipy})(\text{CN})_4]^-$ anion and one $[\text{Mn}^{\text{III}}(\text{salen})]^+$ cation (Fig. 1a). Each $[\text{Fe}(\text{bipy})(\text{CN})_4]^-$ anion coordinates with two $[\text{Mn}^{\text{III}}(\text{salen})]^+$ cations via two *trans*- CN^- groups, whereas each $[\text{Mn}^{\text{III}}(\text{salen})]^+$ cation is linked to two $[\text{Fe}(\text{bipy})(\text{CN})_4]^-$ ions in *trans*-conformation, which results in a straight neutral Fe–Mn bimetallic chain composed of $[\text{Fe}(\text{bipy})(\text{CN})_4]^-$ and $[\text{Mn}(\text{salen})]^+$ alternately linked by the cyanide-bridges (Fig. 1b). As usual, the $[\text{Fe}(\text{bipy})(\text{CN})_4]^-$ fragment exhibits a distorted octahedral structure consisting of two N atoms from a planar bipy and four C atoms from four CN^- groups. The $\text{Fe}-\text{C}\equiv\text{N}$ angles for both terminal $[176.4(2)^\circ$ and $178.5(2)^\circ]$ and bridging $[176.5(2)^\circ$ and $179.1(2)^\circ]$ CN^- are somewhat below that of strict linearity. The $\text{Fe}-\text{C}$ distances for the bridging CN^- $[1.961(2)$ and $1.947(2) \text{ \AA}]$ are slightly longer than those for the ter-

terminal CN^- $[1.917(2)$ and $1.923(2) \text{ \AA}]$, while the C–N distances of the bridging CN^- $[1.140(3)$ and $1.131(3) \text{ \AA}]$ are almost equal to those of the terminal CN^- $[1.140(3)$ and $1.141(3) \text{ \AA}]$. The values of the $\text{Fe}-\text{N}(\text{bipy})$ bond distances $[1.986(2)$ and $1.987(2) \text{ \AA}]$ and that of the angle subtended by the chelating bipy $[80.6(1)^\circ$ at $\text{N}(1)-\text{Fe}(1)-\text{N}(2)]$ are practically the same as those observed in the mononuclear $\text{PPh}_4[\text{Fe}(\text{bipy})(\text{CN})_4]$ and the trinuclear species $\{[\text{Fe}^{\text{III}}(\text{bipy})(\text{CN})_4]_2\text{M}^{\text{II}}(\text{H}_2\text{O})_4\} \cdot 4\text{H}_2\text{O}$ ($\text{M} = \text{Mn}$ or Zn) [22]. The Mn^{III} ion assumes a distorted octahedral coordination geometry, in which the equatorial sites are occupied by N_2O_2 donor atoms of the quadridentate Schiff base ligand salen with the $\text{Mn}-\text{N}/\text{O}$ bond distances of 1.880 – 1.992 \AA , while the axial positions are occupied by two nitrogen atoms from bridging CN^- groups with $\text{Mn}-\text{N}_{\text{ax}}$ distances of 2.282 and 2.329 \AA . The axial elongation accounts for the existence of the well-known Jahn–Teller effect on an octahedral high-spin Mn^{III} ion. The $\text{Mn}-\text{N}\equiv\text{C}$ bond angles deviate significantly from linearity with the angles of $\text{Mn}(1)-\text{N}(7)-\text{C}(29) = 171.3(2)^\circ$ and $\text{Mn}(1\text{B})-\text{N}(8)-\text{C}(30) = 159.6(2)^\circ$. In addition, the bonding parameters of the salen ligand are close to those found in related complexes reported previously [20–21].

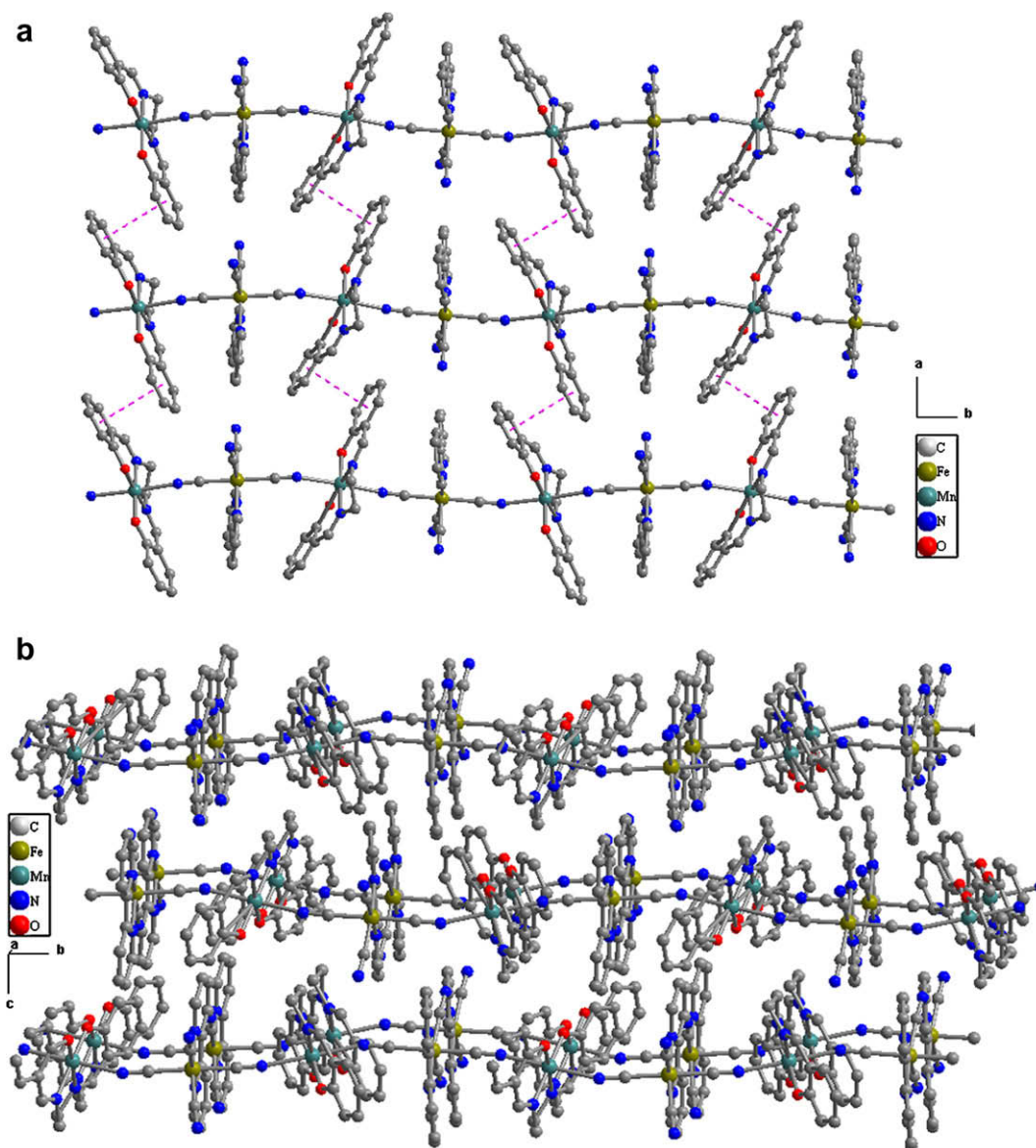


Fig. 2. (a) Projection of complex **1** along the *c*-axis, showing the layer structure. (b) Packing diagram viewed from the *a*-axis.

Table 1
Selected bond distances (Å) and bond angles (°) for complex **1**.

Bond distances			
Fe1–N1	1.9865(18)	Mn1–O1	1.8947(14)
Fe1–N2	1.9868(18)	Mn1–O2	1.8801(14)
Fe1–C27	1.917(2)	Mn1–N3	1.9917(18)
Fe1–C28	1.923(2)	Mn1–N4	1.9803(18)
Fe1–C29	1.947(2)	Mn1–N7	2.2819(17)
Fe1–C30	1.961(2)	Mn1–N8A	2.3292(17)
Bond angles			
N1–Fe1–N2	80.61(7)	N4–Mn1–N8A	89.39(7)
N1–Fe1–C27	97.39(8)	N7–Mn1–N8A	177.29(7)
N1–Fe1–C28	176.18(8)	O1–Mn1–N7	90.97(6)
N1–Fe1–C29	88.74(7)	Mn1B–N8–C30	159.62(17)
N1–Fe1–C30	91.33(7)	Mn1–N7–C29	171.28(17)
N2–Fe1–C27	173.53(7)	Fe1–C27–N5	176.41(19)
N2–Fe1–C28	95.68(8)	Fe1–C29–N7	176.54(18)
N2–Fe1–C29	86.29(7)	Fe1–N1–C1	126.11(16)
N2–Fe1–C30	94.82(7)	Fe1–N1–C5	115.39(14)
C27–Fe1–C28	86.20(9)	Fe1–N2–C6	115.50(14)
C27–Fe1–C29	87.52(8)	Fe1–N2–C10	125.18(16)
C27–Fe1–C30	91.37(8)	Fe1–C28–N6	178.54(19)
C28–Fe1–C29	90.10(8)	Fe1–C30–N8	179.09(18)
C28–Fe1–C30	89.90(8)		
C29–Fe1–C30	178.89(8)		

Symmetry transformations used to generate equivalent atoms: $A = 1 - x, -1/2 + y, 3/2 - z$; $B = 1 - x, 1/2 + y, 3/2 - z$.

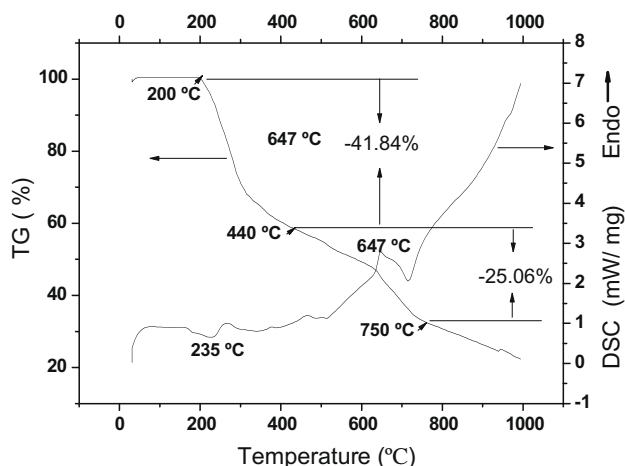


Fig. 3. TG-DSC curves of complex **1**.

The intrachain Fe \cdots Mn distances through the CN $^-$ bridges are 5.336 and 5.351 Å, which is somewhat agreement with that of the Fe–Mn system with mpzccq and pzcq [24–25]. The nearest interchain Fe \cdots Mn, Mn \cdots Mn and Fe \cdots Fe distances is 6.771, 6.513 and 7.288 Å. It is known that the packing of the bimetallic chains is often dominated by aromatic π – π stacking interactions in the case of the presence of large aromatic ligands [21]. The chains in complex **1** are running along the b direction, and form layers parallel to the ab plane. In the layer each chain interacts with two other adjacent chains via face-to-face π – π stacking between the benzene rings of the salen ligand of the [Mn(salen)] $^+$ units (Fig. 2a). The plane-to-plane distance is 3.81 Å, and the dihedral angle is 7°. The adjacent chains are also held together by the weak H-bonds between the terminal cyanides of [Fe(bipy)(CN) $_4$] $^-$ units in one chain and the C–H donors of bipy ligands in neighboring chains. The 3D structure is formed by the layers stacking along c direction mainly via van der Waals interaction (Fig. 2b).

3.2. Thermal analysis

The thermoanalysis was performed in nitrogen atmosphere with a heating rate of 10 °C min $^{-1}$. Fig. 3 shows the TG–DSC curve of complex **1**. With increasing temperature, the complex can keep stable until 200 °C. After that, the complex starts to decompose with a series of continuous weight loss processes. The weight loss of 41.84% from 200 to 440 °C is consistent with the loss of the ligand salen (calcd. 41.78%). The following weight loss of 25.06% from 440 to 750 °C might be due to the loss of the ligand bipy (calcd. 24.51%). When further heating, the decomposition continues with further weight loss.

3.3. Magnetic properties

The magnetic susceptibilities of complex **1** were measured with an applied field $H = 2$ kOe in the temperature range 1.8–300 K. The plots of $\chi_M T$ vs. T and $1/\chi_M$ vs. T are given in Fig. 4. At room temperature, the $\chi_M T$ per MnFe unit is 3.49 emu K mol $^{-1}$ (5.28 μ_B), which is consistent with the spin-only value of 3.38 emu K mol $^{-1}$ (5.2 μ_B) expected for an uncoupled spin system (one $S_{Fe} = 1/2$, one $S_{Mn} = 2$) with $g = 2.0$. On lowering the temperature, the $\chi_M T$ value almost keeps constant until 60 K, then gradually decreases to 3.0 emu K mol $^{-1}$ (4.9 μ_B) at 14 K, finally sharply decreases with further decreasing temperature to 1.62 emu K mol $^{-1}$ (3.6 μ_B) at 1.8 K. The plot of $1/\chi_M$ vs. T obeys the Curie–Weiss law with a negative Weiss constant $\theta = -2.6$ K. These results indicate the presence of a weak antiferromagnetic interaction in complex **1**, which can be attributed to antiferromagnetic coupling between Fe III and Mn III ions through cyanide-bridges. The field dependence of the magnetization measured at 1.8 K is shown in Fig. 5. The magnetization cannot reach saturation until 70 kOe. The experimental curve is always lower than that derived from the Brillouin function at 1.8 K, confirming further antiferromagnetic coupling between the adjacent Fe III and Mn III . The antiferromagnetic interaction between the Mn III ($S = 2$) and Fe III ($S = 1/2$) can be rationalized in terms of the overlap of the magnetic orbitals of these ions [5]. It is interesting to note that the magnetism of complex **1** is obviously different from that of its Cr III –Mn III analogs [21], which are metamagnets showing antiferromagnetic to ferrimagnetic transition due to strong intrachain uncompensated antiferromagnetic coupling and weak interchain antiferromagnetic coupling. In Cr $^{III}(t_{2g}^3 e_g^0)$ –Mn $^{III}(t_{2g}^3 e_g^1)$ there are nine antiferromagnetic exchanging approaches via electrons in the $t_{2g}(\text{Cr})$ and $t_{2g}(\text{Mn})$ orbitals, while in the situation of Fe $^{III}(t_{2g}^5 e_g^0)$ –Mn $^{III}(t_{2g}^3 e_g^1)$ here there are only one-third the antiferromagnetic approaches as the Cr III –Mn III pair has

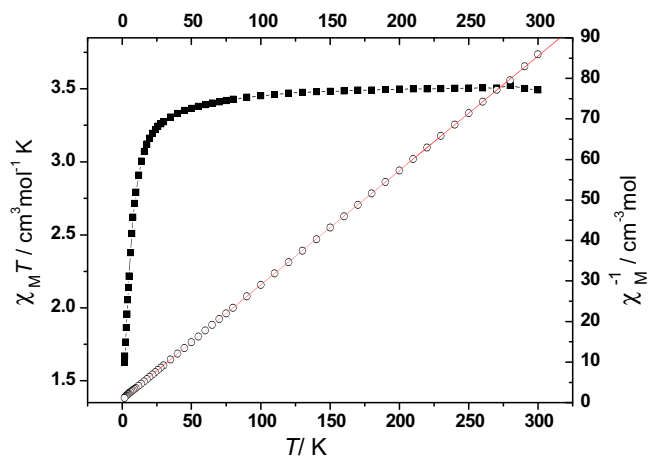


Fig. 4. Temperature dependence of $\chi_M T$ (■) and $1/\chi_M$ (○) for complex **1** measured at 2 kOe. The solid line represents the fit obtained by the Curie–Weiss law (see text).

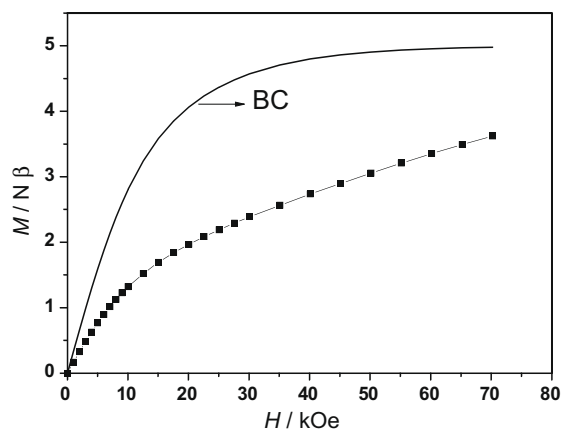


Fig. 5. Field dependence of the magnetization for **1** at 1.8 K. The Brillouin curve (BC) for the independent one Fe^{III} and one Mn^{III} ions is given at 1.8 K.

because there is only one unpaired electron in the t_{2g} orbitals of Fe^{III}. Therefore, the Fe^{III}–Mn^{III} antiferromagnetic coupling in complex **1** is much weaker than the Cr^{III}–Mn^{III} antiferromagnetic coupling in the Cr^{III}–Mn^{III} analogs and, as a result, unlike the Cr^{III}–Mn^{III} analogs, complex **1** cannot form the ferrimagnetic chains. Of course, it is possible that there exists a very weak interchain antiferromagnetic interaction in complex **1**, which might contribute to the overall antiferromagnetic property of this complex [21]. Furthermore, complex **1** also supplies an additional example confirming that the substitution of Cr^{III} with Fe^{III} will result in a weaker magnetic coupling in cyanide-bridged bimetallic systems [5].

4. Conclusion

A new cyano-bridged bimetallic assembly, [Mn(salen)]Fe(bipy)(CN)₄, has been synthesized and characterized structurally and magnetically. This complex has a straight chain structure as the [Fe(bipy)(CN)₄][−] unit, with its two *trans*-cyanide ligands, connects the two neighboring [Mn(salen)]⁺ units at axial positions. The chains stack via mainly the aromatic π – π -type interactions. The complex shows a weak antiferromagnetic interaction between the adjacent Fe^{III} and Mn^{III} ions through cyanide-bridges. The present example further demonstrates [Fe(bipy)(CN)₄][−] as an effective building block in constructing cyano-bridged low-dimensional systems. The synthetic approach can be extended to explore bimetallic systems with other transition metals, and this may bring about a deeper understanding of the magnetic interaction in molecule-based magnetic materials.

5. Supplementary materials

CCDC 709293 contains the supplementary crystallographic data for this paper. These data can be obtained free of charge via <http://www.ccdc.cam.ac.uk/conts/retrieving.html> (or from the Cambridge Crystallographic Data Centre, 12, Union Road, Cambridge CB2 1EZ, UK; fax: +44 1223 336033).

Acknowledgments

Thanks for financial support from the Foundation of State Key Laboratory of Coordination Chemistry and the National Natural Science Foundation of China (No. 20875039).

References

- [1] C.T. Chen, K.S. Suslick, *Coord. Chem. Rev.* 128 (1993) 293.
- [2] H. Oshio, M. Nihei, S. Koizumi, T. Shiga, H. Nojiri, M. Nakano, N. Shirakawa, M. Akatsu, *J. Am. Chem. Soc.* 127 (2005) 4568.
- [3] A.J. Tasiopoulos, W. Wernsdorfer, B. Moulton, M.J. Zaworotko, G. Christou, *J. Am. Chem. Soc.* 125 (2003) 15274.
- [4] W.W. Ni, Z.H. Ni, A.L. Cui, X. Liang, H.Z. Kou, *Inorg. Chem.* 46 (2007) 22.
- [5] M. Verdaguer, A. Bleuzen, V. Marvaud, J. Vaissermann, M. Seuleiman, C. Desplanches, A. Scullier, C. Train, R. Garde, G. Gelly, C. Lomench, I. Rosenman, P. Veillet, C. Cartier, F. Villain, *Coord. Chem. Rev.* 190–192 (1999) 1023.
- [6] M. Ohba, H. Okawa, *Coord. Chem. Rev.* 198 (2000) 313.
- [7] J. Cernak, M. Orendac, I. Potocnak, J. Chomic, A. Orendacova, J. Skorsepka, A. Feher, *Coord. Chem. Rev.* 224 (2002) 51.
- [8] H.R. Wen, C.F. Wang, J.L. Zuo, Y. Song, X.R. Zeng, X.Z. You, *Inorg. Chem.* 45 (2006) 582.
- [9] R. Lescouëzec, F. Lloret, M. Julve, J. Vaissermann, M. Verdaguer, R. Llusar, S. Uriel, *Inorg. Chem.* 40 (2001) 2065.
- [10] S. Wang, M. Ferbinteau, M. Yamashita, *Inorg. Chem.* 46 (2007) 610.
- [11] P.A. Berseth, J.J. Sokol, M.P. Shores, J.L. Heinrich, J.R. Long, *J. Am. Chem. Soc.* 122 (2000) 9655.
- [12] F. Karadas, E.J. Schelter, A.V. Prosvirin, J. Bacska, K.R. Dunbar, *Chem. Commun.* (2005) 1414.
- [13] S. Wang, J. Zuo, L.H.C. Zhou, H.J. Choi, Y.X. Ke, J.R. Long, X.Z. You, *Angew. Chem. Int. Ed.* 43 (2004) 5940.
- [14] E.J. Schelter, A.V. Prosvirin, K.R. Dunbar, *J. Am. Chem. Soc.* 126 (2004) 15004.
- [15] D.F. Li, S. Parkin, G.B. Wang, G.T. Yee, A.V. Prosvirin, S.M. Holmes, *Inorg. Chem.* 44 (2005) 4903.
- [16] R. Lescouëzec, L.M. Toma, J. Vaissermann, M. Verdaguer, F.S. Delgado, C. Ruiz-Pérez, F. Lloret, M. Julve, *Coord. Chem. Rev.* 249 (2005) 2691.
- [17] H. Miyasaka, H. Ieda, N. Matsumoto, N. Re, R. Crescenzi, C. Floriani, *Inorg. Chem.* 37 (1998) 255.
- [18] H. Miyasaka, N. Matsumoto, H. Okawa, N. Re, E. Gallo, C. Floriani, *J. Am. Chem. Soc.* 118 (1996) 981.
- [19] H.J. Choi, J.J. Sokol, J.R. Long, *Inorg. Chem.* 43 (2004) 1606.
- [20] X.P. Shen, B.L. Li, J.Z. Zou, H. Hu, Z. Xu, *J. Mol. Struct.* 657 (2003) 325.
- [21] F. Pan, Z.M. Wang, S. Gao, *Inorg. Chem.* 46 (2007) 10221.
- [22] R. Lescouëzec, F. Lloret, M. Julve, J. Vaissermann, M. Verdaguer, *Inorg. Chem.* 41 (2002) 818.
- [23] N. Matsumoto, N. Takemoto, A. Ohyoshi, H. Okawa, *Bull. Chem. Soc. Jpn.* 61 (1988) 2984.
- [24] J.I. Kim, H.S. Yoo, E.K. Koh, C.S. Hong, *Inorg. Chem.* 46 (2007) 10461.
- [25] J.I. Kim, H.S. Yoo, E.K. Koh, H.C. Kim, C.S. Hong, *Inorg. Chem.* 46 (2007) 8481.